UNITED STATES DEPARTMENT OF THE INTERIOR
GEOLOGICAL SURVEY

Earthquake Hazards in the Pacific Northwest of the United States

Compiled by
A. M. Rogers
T. J. Walsh
W. J. Kockelman
G. R. Priest

ENGINEERING CHARACTERIZATION OF EARTHQUAKE STRONG GROUND MOTIONS WITH APPLICATIONS TO THE PACIFIC NORTHWEST

By Walter J. Silva,[1] Ivan G. Wong[1] and Robert B. Darragh[1,2]

Open-File Report 91-441-H

1991

---

[1] Woodward-Clyde Consultants, 500 12th Street, Oakland, CA 94607.
[2] Now at California Division of Mines and Geology, Sacramento, CA 95816.

Foreword

This paper is one of a series dealing with earthquake hazards of the Pacific Northwest, primarily in western Oregon and western Washington. This research represents the efforts of U.S. Geological Survey, university, and industry scientists in response to the Survey initiatives under the National Earthquake Hazards Reduction Program. Subject to Director's approval, these papers will appear collectively as U.S. Geological Survey Professional Paper 1560, tentatively titled "Assessing and Reducing Earthquake Hazards in the Pacific Northwest." The U.S. Geological Survey Open-File series will serve as a preprint for the Professional Paper chapters that the editors and authors believe require early release. A single Open-File will also be published that includes only the abstracts of those papers not included in the pre-release. The papers to be included in the Professional Paper are:

Introduction

Rogers, A.M., Walsh, T.J., Kockelman, W.J., and Priest, G.R., "Assessing and reducing earthquake hazards in the Pacific Northwest: An overview

Tectonic Setting

Paleoseismicity

Adams, John, "Great earthquakes recorded by turbidites off the Oregon-Washington margin"

Atwater, Brian, "Coastal evidence for great earthquakes in western Washington"

Nelson, Alan R. and Personius, Stephen F., "The potential for great earthquakes in Oregon and Washington: An overview of recent coastal geologic studies and their bearing on segmentation of Holocene ruptures, central Cascadia subduction zone"

Peterson, C. D. and Darienzo, M. E., "Discrimination of climatic, oceanic, and tectonic forcing of marsh burial events from Alsea Bay, Oregon, U.S.A."

Tectonics/Geophysics

Goldfinger, C. Kulm, V., Yeats, R., Appelgate, B., MacKay, M., and Cochrane, G., "Active strike slip faulting and folding in the Cascadia plate boundary and forearc, in central and northern Oregon"

Ma, Li, Crosson, Robert, and Ludwin, Ruth, "Focal mechanisms of western Washington earthquakes and their relationship to regional tectonic stress"

Snavely, P. D., Jr., "Cenozoic evolution of the continental margin of Oregon and Washington"

Weaver, C. S. and Shedlock, K. M., "Estimates of seismic source regions from considerations of the earthquake distribution and regional tectonics"

Yeats, Robert, Graven, E.P., Werner, K.S., Goldfinger, C., and Popowski, T, "Tectonic setting of the Willamette Valley, Oregon"

Earthquake Hazards

Ground Motion Prediction

Cohee, B.P., Somerville, P.G., Abrahamson, N.A., "Ground motions from simulated Mw=8 Cascadia earthquakes"

King, Kenneth, Carver, D., Williams, R., Worley, D., "Site response studies in west and south Seattle, Washington"

Madin, Ian P., "Earthquake-hazard geology maps of the Portland metropolitan area, Oregon"

Silva, Walter, Wong, Ivan, and Darragh, Robert, "Engineering characterization of strong ground motions with applications to the Pacific Northwest"

Ground Failure

Chleborad, A. F. and Schuster, R. L., "Earthquake-induced ground failure associated with the April 13, 1949, and April 29, 1963, Puget Sound area, Washington, earthquakes"

Grant, W. P., Perkins, W. J., and Youd, L., "Liquefaction susceptibility maps for Seattle, Washington North and South Quadrangles

Earthquake Risk Assessment

Wang, Leon R.L., Wang, Joyce C.C., and Ishibashi, Isao, "GIS applications in seismic loss estimation model for Portland, Oregon water and sewer systems"

Implementation

Kockelman, William J., "Techniques for reducing earthquake hazards--An introduction"

Booth, Derek B. and Bethel, John, "Approaches for seismic hazard mitigation by local governments--An example from King County, Washington"

May, P.J., "Earthquake risk reduction prospects for the Puget Sound and Portland Areas"

Perkins, J.B. and Moy, K.K., "Liability for earthquake hazards or losses and its impacts on Washington's cities and counties"

Preuss, Jane and Hebenstreit, G. T., "Integrated hazard assessment for a coastal community: Grays Harbor"

Contents

List of Tables

Illustrations

ABSTRACT

Strong ground motion estimates in terms of acceleration response spectra for the 1949 M 7.1 Olympia and 1965 M 6.5 Seattle-Tacoma earthquakes have been computed based on the Band-Limited-White-Noise earthquake source model coupled with random vibration theory. These estimates compare favorably with the actual recordings. Acceleration response spectra and time histories for a hypothetical M 8 Cascadia subduction zone earthquake have also been predicted for a hard rock and deep soil site in Seattle at a rupture distance of 70 km (43.8 mi). The estimated peak horizontal ground accelerations are 0.11 and 0.17 g, respectively. Based on our analysis, the effects of near-surface soils and the properties of the underlying rock will likely be significant factors controlling strong ground motions in the Puget Sound region and, similarly, the Willamette Valley region of the Pacific Northwest.

INTRODUCTION

An essential element in the seismic design of engineered structures is a quantitative estimate of the characteristics of strong ground motion. Of particular importance is a specification of the peak levels of ground motion, as well as spectral content, as characterized by response spectra or power spectral density. The spectral content is reasonably well defined for shallow earthquakes occurring in western North America with approximate moment magnitudes (M) 6 to 7 (Mohraz, 1976; Seed et al., 1976; Joyner and Boore, 1988). However, recent observations of strong ground motions in other tectonic regimes have revealed significant differences in the spectral content of earthquakes recorded at rock sites. Ground motions recorded in stable tectonic regimes typical of eastern North America (ENA) may have significantly higher frequency content and larger peak values than corresponding motions typical of active regimes like western North America (WNA) (Boore and Atkinson, 1987; Toro and McGuire, 1987; Silva et al., 1989; Silva and Darragh, 1990).

A relatively new earthquake source model which is extremely simple in concept, called the Band-Limited-White-Noise (BLWN) model combined with random vibration theory (RVT) has been remarkably successful in predicting peak ground motion values as well as spectral ordinates in different tectonic regimes (Hanks and McGuire, 1981; Boore, 1983; Boore and Atkinson, 1987). The BLWN-RVT methodology has been applied to a worldwide data set of earthquakes ranging from M 1.5 to 8.1 in an analysis of rock motions recorded at distances generally less than 50 km (Silva and Darragh, 1990). This study has shown that the controlling factors in the specification of strong ground motion for engineering design are the moment magnitude, source distance, and the rock properties directly beneath the site extending to depths of approximately several hundred meters to 2 km (1.3 mi). Specifically, the near-surface attenuation modeled through the parameter kappa (κ) exerts a predominate effect upon spectral composition for frequencies beyond approximately 3 Hz. Below this frequency range, M or seismic moment through corner frequency (see equation 3) controls spectral shapes in the BLWN-RVT ground motion methodology.

Of particular interest to seismic hazards in the Pacific Northwest, is the possibility of a great Cascadia subduction zone earthquake ($M > 8$) occurring beneath western Washington and Oregon. While the source processes of such earthquakes may, in detail, be different from intraplate and non-subduction interplate events, our analyses suggest that the simple BLWN-RVT model can accurately predict the spectral content of such events for engineering design. Four earthquakes, including the 19 September 1985 M 8.1 Michoacan mainshock, which occurred in the subduction zone along the coast of western Mexico and were recorded by the Guerrero strong motion network have been modeled quite well for periods of 0.03 to 4 sec and at distances to the rupture surface as close as 16 km (10.0 mi) (Silva and Darragh, 1990) (see further discussion). Thus for both interplate and intraplate earthquakes, the controlling factor in ground motions for engineering design at rock sites, as previously stated, appears to be the rock characteristics directly beneath the site, specifically the density, shear-wave velocity, and the quality factor Q or attenuation.

An additional advantage of the BLWN-RVT methodology is the ability to easily incorporate site-specific non-linear soil response directly into the ground motion analyses using RVT and the plane-wave propagators of Silva (1976) in an equivalent-linear formulation. This is an important consideration in seismic hazard evaluations in the Pacific Northwest because of the widespread existence of alluvial deposits beneath many of the urban areas.

In this study, we have applied the BLWN-RVT methodology to generate acceleration response spectra to compare with the 1949 M 7.1 Olympia and 1965 M 6.5 Seattle-Tacoma earthquakes as recorded by the strong motion instruments located in the Highway Test Office (OHT) in Olympia and the Federal Office Building (FED) in Seattle (1965 earthquake only). Both earthquakes occurred within the subducting Juan de Fuca plate. Incorporating site-specific shear-wave velocity and density data in geologic profiles beneath these two sites and the source parameters of the two earthquakes, we have been able to match quite well the average response spectral shapes computed from the actual strong ground motion recordings. Predicted accelerograms and acceleration response spectra for a postulated M 8 Cascadia subduction zone earthquake have also been generated for the FED site and a hypothetical hard rock site in Seattle.

METHODOLOGY AND ANALYSIS

BLWN-RVT 5% damped median response spectral shapes are computed from the acceleration spectral density a(f) to compare with the shapes computed from actual strong motion recordings. The acceleration spectral density (fig. 1) is given by

$$a(f) = C \frac{f^2}{1+(f/f_c)^2} \frac{M_o}{R} P(f) A(f) e^{-\frac{\pi f R}{\beta_o Q(f)}} \quad (1)$$

where

M_o	seismic moment
R	distance to the equivalent point source
β_o	shear wave velocity at the source
ρ_o	density at the source
Q(f)	frequency dependent quality factor
A(f)	near-surface amplification factors (Boore, 1986)
P(f)	high-frequency truncation filter
f_c	source corner frequency and

$$C = (1/\rho_o\beta_o^3) \cdot (2) \cdot (0.63) \cdot (1/\sqrt{2}) \cdot \pi \quad (2)$$

C is a constant which contains ρ_o and β_o terms and accounts for the free-surface effect (factor of 2), the source radiation pattern averaged over a sphere (0.63) (Boore, 1983), and the partition of energy into two horizontal components $(1/\sqrt{2})$.

Source scaling is provided by specifying two independent parameters: the seismic moment (M_o) and the high-frequency stress parameter ($\Delta\sigma$) (fig. 1). The stress parameter is taken to be independent of magnitude (Atkinson, 1984; Boore and Atkinson, 1987; Toro and McGuire, 1987) and relates the corner frequency f_c to M_o through the relation

$$f_c = \beta_o(\Delta\sigma/8.44\ M_o)^{1/3} \quad (3)$$

The spectral shape of the single-corner-frequency ω-square source model is then described by the two free parameters, M_o and $\Delta\sigma$. The corner frequency increases with the shear-wave velocity and stress parameter,

both of which are region dependent. The near-surface amplification factors that account for the increase in amplitude as the seismic energy travels through lower velocity crustal rocks near the surface are taken from Boore (1986).

The P(f) filter is an attempt to model the observation that acceleration spectral density appears to fall off rapidly beyond some region-dependent maximum frequency. This observed phenomenon truncates the high frequency portion of the spectrum and is responsible for the band-limited nature of the model. This spectral fall-off has been attributed to near-site attenuation (Hanks, 1982; Anderson and Hough, 1984) or to source processes (Papageorgiou and Aki, 1983) or perhaps to both effects. In the Anderson and Hough (1984) attenuation model, the form of the P(f) filter is taken as

$$P(f) = e^{-\pi\kappa f} \tag{4}$$

At zero epicentral distance

$$\kappa(0) = \frac{H}{\overline{\beta_s}\,\overline{Q_s}} \tag{5}$$

The bar in equation 5 represents an average of these quantities over a depth H beneath the recording site. The value of $\kappa(0)$ is attributed to attenuation in the very shallow crust directly below the site (Hough et al., 1988). The intrinsic attenuation along this part of the path is not thought to be frequency dependent and is modeled as a frequency independent, but site-dependent constant κ (Hough et al., 1988). κ has been determined for several rock and soil sites representative of WNA (Anderson and Hough, 1984; Anderson, 1986). For a WNA competent rock site, a value in the range of 0.02 to 0.03 sec is appropriate (Silva et al., 1989; Silva and Darragh, 1990).

The path attenuation from the source to just below the site is modeled with the frequency-dependent quality factor Q(f). The Q(f) models are based upon analyses of attenuation in WNA by Nuttli (1986). These models along with the remaining parameters considered to be representative of the Pacific Northwest are shown in table 1.

The Fourier amplitude spectrum given by equation 1 for a(f) represents the BLWN source model employing a Brune spectrum that is characterized by a single corner frequency. It is appropriate for a point source and models direct shear-waves in a homogeneous half-space (with effects of a velocity gradient through the A(f) filter). For vertically inhomogeneous layered structures, the plane-wave propagators of Silva (1976) are used to propagate S_H motion through the layered structure. Effects due to source finiteness as well as two-dimensional propagation path complexities do not appear to significantly affect spectral shapes for subduction earthquakes up to M 8.1 and for epicentral distances ranging from 20-166 km (6.1-50.6 mi) (Silva and Darragh, 1990). Figure 2 showing the good agreement between the BLWN-RVT computed and observed spectral shapes of the M 7.9 Michoacan earthquake at a distance of 16 km illustrates this point very well. (The response spectral shapes shown in this paper are computed by dividing the response spectra by the peak ground acceleration. Such spectral shapes provide a convenient and an appropriate normalization for distance [Silva and Green, 1989]). For estimates of peak acceleration for subduction earthquakes, however, path complexities may result in departures from homogeneous half-space assumptions and, for these cases, the BLWN-RVT spectral shape can be scaled to empirical predictions.

In order to compute peak time domain values, that is peak acceleration and peak oscillator response, RVT is used to relate rms computations to peak value estimates (Boore, 1983; Boore and Joyner, 1984). The procedure, in general, involves computing the rms value by integrating the power spectrum from zero to the

Nyquist frequency and applying Parseval's relation. Extreme value theory is then used to estimate the expected ratio of the peak value to the rms value of a specified duration of the BLWN time history. The duration is generally taken as the inverse of the corner frequency (Boore, 1983).

Soil Response

In order to accommodate the effects of site-specific soil response, the BLWN power spectrum of the rock outcrop motion is propagated through the one-dimensional soil profile using the plane-wave propagators of Silva (1976). In this formulation only SH waves are considered. Arbitrary angles of incidence may be specified but normal incidence is used throughout the present analyses. In order to treat possible material nonlinearities, the equivalent-linear formulation is employed. RVT is used to predict peak time domain values of shear-strain based upon the shear-strain power spectrum. In this sense, the procedure is analogous to the program SHAKE except that peak shear strains in SHAKE are measured in the time domain. The purely frequency domain approach obviates a time domain control motion and perhaps, just as significantly, eliminates the need for a suite of analyses based on different input motions. This arises because each time domain analysis may be viewed as one realization of a random process. In this case, several realizations of the random process must be sampled to have a statistically stable estimate of site response. The realizations are usually performed by employing different control motions with approximately the same level of peak acceleration. In the case of the frequency domain approach, the estimates of peak shear strain as well as oscillator response are, as a result of RVT, fundamentally probabilistic in nature. Stable estimates of site response can then be easily computed. The procedure of generating the BLWN power spectrum, computing the equivalent-linear layered-soil response, and estimating peak time domain values has been incorporated into a single computer code which accommodates up to 3000 constant velocity layers. This capability allows modeling of upper crustal layers as well as smooth velocity gradients.

Comparison of RVT Estimates with SHAKE

In order to demonstrate the appropriateness of site response computations using the frequency domain approach with RVT estimates of ground motion as well as oscillator response, a comparison with results from SHAKE is presented. The soil profile used for the comparison is shown in figure 3 and consists of a 120-foot (36.6 m) thick stiff sand profile over rock. The modulus reduction and damping curves used in the analysis are shown in figure 4. The variation of shear modulus with strain is taken as the upper range Seed and Idriss (1970) sand curve. The upper range was chosen as recent work on observations of site response (Silva et al., 1987) indicated that in situ soil response to earthquake motions showed less shear-strain dependency of shear modulus than that predicted by the mid-range values. The damping curve used departs from the mid-range values at low strains to accommodate observations of shear-wave damping for wave propagation at low levels of motion (Joyner et al., 1976; Joyner et al., 1981; Johnson and Silva, 1981). These observations show low-strain damping values around 2% of critical rather than the 0.5 to 1% resulting from laboratory analyses. The lower shear-wave damping for wave propagation at high levels is an attempt to reconcile observations of higher peak acceleration values at deep soil sites from the 1979 Imperial Valley earthquake than would be expected from predictions using the mid-range curve.

Figure 5 shows the input and output time histories resulting from the SHAKE and RVT analysis. The synthetic time history of the outcrop motion is computed by combining the BLWN Fourier spectrum for a M 6.5 event at a hypocentral range of 8.5 km (5.3 mi) with the phase spectrum of an observed event. This motion is used as the rock outcrop or control motion input to SHAKE to produce a time history (fig. 5). The filtering effects of the soil column are easily seen with little effect on peak acceleration. Apparently, in this case, the amplification of the soil profile for frequencies associated with the peak acceleration is compensated by the damping. For the RVT analysis, the power spectrum of the input time history is used as input. The output time history is generated by combining the Fourier spectrum at the surface of the site with the phase spectrum from the outcrop motion (fig. 5). The two outputs, SHAKE and the RVT, are nearly indistinguishable. This indicates that the two approaches in estimating peak shear strains, time domain and RVT, result in very nearly the same

values with depth. Of particular note, the peak acceleration at the surface of the profile predicted by the RVT is 1.0 g which is quite close to the 0.96 g value resulting from the SHAKE analysis.

The 5% damped absolute acceleration response spectra of the control motion, SHAKE output, and the RVT analysis output are shown in fig. 6. The smooth response spectra for the rock motion and for the surface of the soil are the RVT estimates of oscillator response. The time domain (SHAKE) results are rather oscillatory, due to the phase spectrum (Silva and Green, 1988), but generally follow the RVT. Figure 6 clearly demonstrates the necessity in averaging several time domain results, experimental or computational, in order to produce stable estimates of site response.

DATA

The 1949 (surface wave magnitude M_s 7.1, M 7.1) Olympia earthquake occurred at a depth of 49 km (30.6 mi) and at an epicentral distance of approximately 5 km (3.1 mi) from OHT (Baker and Langston, 1987). Peak horizontal ground accelerations of 0.16 and 0.28 g and peak horizontal velocities of 17.0 and 21.4 cm/sec were recorded at OHT (Earthquake Engineering Research Laboratory, 1973). The 1965 (M_s 6.5, M 6.5) Seattle-Tacoma earthquake occurred at a depth of 60 km (37.5 mi) and at epicentral distances of 21 and 69 km (13.1 and 43.1 mi) from FED and OHT, respectively (Langston and Blum, 1977; Langston, 1981; Ihnen and Hadley, 1986). Peak horizontal accelerations of 0.067 and 0.068 g and peak velocities of 7.9 and 8.2 cm/sec were recorded at FED (Earthquake Engineering Research Laboratory, 1973). Values of 0.14 and 0.20 g and 8.0 and 12.7 cm/sec were recorded at OHT.

The input parameters that are required for the BLWN-RVT methodology are: (1) the source parameters of the earthquake including the seismic moment or moment magnitude and stress parameter; (2) shortest distance to the fault rupture plane; (3) propagation path parameters (assuming a half-space) including the shear wave velocity (β_s), density (ρ), and the quality factor Q_o and η which describe the frequency-dependent path attenuation; and (4) the site parameters, β_s, Q_s and ρ, specified as a function of depth as well as appropriate modulus reduction and damping curves.

The stress parameter was assumed to be 100 bars for large earthquakes in the Pacific Northwest (C. Langston, Pennsylvania State University, personal communication, 1989). Although Boore (1986) determined that a value of 50 bars gave a good fit to matching the peak accelerations and velocities of 19 earthquakes ranging from M 6.5 to 9.5 (of which the majority were subduction zone earthquakes), the use of 100 bars is within the reasonable range of dynamic stress drops and appears to fit the observed data well (see following discussion).

The propagation path was characterized by a β of 3.2 km/sec (2.0 mi/sec), Q_o of 150, η of 0.6 and ρ of 2.7 g/cm^3 based on standard values for western North America (Silva and Darragh, 1990). Geologic profiles for the two sites, OHT and FED are shown in figure 7 based on Washington Public Power Supply System (1974, 1986) and Shannon and Wilson, Inc. and Agbabian Associates (1978). At OHT, a 156-m (512 ft) deep borehole was almost entirely within glacial sediments. Low-strain shear-wave velocities ranged from 142 m/sec (467 ft/sec) at the surface to 685 m/sec (2247 ft/sec) at a depth of 131 m (430 ft). At FED, fill material was encountered to a depth of 7 m (23 ft). The natural soils at the site have velocities ranging from 198 to 1006 m/sec (649 to 3300 ft/sec) to a depth of 122 m (400 ft). Dynamic soil properties at the sites shown in figure 4 were used.

RESULTS AND DISCUSSION

The comparison of the response spectral shapes computed from the recorded data to shapes computed from the BLWN-RVT model are shown in figures 8 to 10. In all cases, the predictions of the BLWN-RVT ground motion model capture the general features of the spectral shapes calculated from the data between 0.2 to 33 Hz quite well. The overall shape, frequency, and level of maximum spectral amplification and peak

ground acceleration compare favorably with the recorded values at these two sites (table 2). The model, however, underpredicts by a factor of approximately two the peak acceleration at OHT for the 1965 earthquake. This discrepency is also observed in the work of Langston (1981) and Shakal and Toksoz (1980) who suggest that higher values of Q are characteristic of the OHT site compared to the FED site. More detailed borehole and upper crustal information on β and Q are needed to resolve this inconsistency.

Ground motions were computed for the FED site from a M 8.0 Cascadia earthquake at a hypocentral distance of 70 km (43.8 mi) (fig. 11). The median peak ground acceleration and velocity estimated by the BLWN-RVT model are 0.165 g and 19.3 cm/sec, respectively (table 2). The bracketed duration of strong shaking (Bolt, 1973) in excess of 0.10 g is about 20 seconds. For comparison, the ground motions for a hypothetical hard rock site (the FED geologic profile without the soil) for a M 8 earthquake at the same hypocentral distance of 70 km (43.8 mi) were also estimated. The corresponding values are 0.105 g and 14.8 cm/sec (table 2). Figure 11 shows the 5% damped absolute acceleration response spectra for these two cases. The dramatic effect of the soil site is clear. The FED site has an increased response compared to the rock response for periods between 0.2 and 3 sec. This is also evident in the synthetic accelerograms which exhibit higher levels of ground motion and a lower frequency content for the FED site (fig. 12). The high frequency ground motions from 0.05 to 0.2 sec at the FED site are, however, actually lower than the rock site due to deamplification resulting from the damping in the soil response.

The absolute acceleration spectra (fig. 11) are computed from the predicted accelerograms shown in figure 12. The accelerograms are produced by combining the BLWN amplitude spectra estimated with the above parameters with a phase spectrum from an observed strong ground motion recording using the technique described by Silva and Lee (1987). The two most important criteria in selecting the phase from a recorded earthquake for the hypothetical event are that the seismic moment (or M) and the source-to-site distance should be comparable. These criteria produce synthetic records with appropriate durations and timing of the major phase arrivals so that the distribution of energy with time in the synthetic record appears reasonable. Time histories produced in this manner are not intended to represent an extension of the BLWN methodology nor are they viewed as results of detailed modeling. Rather such time histories are intended to approximate expected durations. As such, they are appropriate for non-linear analyses of structures as well as embankments and soil profiles for failure.

To satisfy the above criteria, an accelerogram recorded at La Union during the 1985 Michoacan earthquake was selected. This earthquake had a M_o estimated at 10.3×10^{27} dyne-cm and a fault rupture area of approximately 170 by 50 km (106.3 by 31.3 mi) (Anderson et al., 1986; 1987). These parameters compare favorably with our hypothetical Cascadia earthquake source parameters. The site geology at La Union, a meta-andesite basalt (Anderson et al., 1987), is also comparable to the hard rock site conditions used in the BLWN-RVT modeling.

Secondly, the strong motion instrument at La Union was located 121 km (75.6 mi) from the epicenter but directly above the aftershock zone and the inferred rupture area of the mainshock. The average distance from the earthquake source to La Union is approximately 60 km (37.5 mi) which is comparable to the 70 km (43.8 mi) source-to-site distance used for the Cascadia earthquake ground motion estimates. Thus, the phase from the La Union accelerogram is probably an appropriate description of the distribution of energy with time for a postulated M 8 Cascadia earthquake.

SUMMARY

Estimates of the acceleration response spectral shapes and peak values for the 1949 and 1965 earthquakes based on the BLWN-RVT ground motion methodology compare favorably with actual recordings at OHT and FED. The methodology also predicts median estimates of peak horizontal acceleration and peak horizontal velocity of 0.17 g and 19.3 cm/sec, respectively, for the FED site in downtown Seattle and 0.11 g and 14.8 cm/sec for a hypothetical hard rock site from a postulated M 8.0 Cascadia subduction zone earthquake

at a distance of 70 km (43.8 mi). The need for more site-specific studies is exemplified by the observation that the site response at OHT and at the hypothetical hard rock site differs significantly from the site response at FED. Based on this analysis, the effects of near-surface soils and the properties of the underlying rock may likely exert a dominant influence on strong ground motion in the Puget Sound region and possibly the Willamette Valley in Oregon.

ACKNOWLEDGMENTS

This study was supported by the Professional Development Program of Woodward-Clyde Consultants. Our appreciation to John Bischoff and Jack O'Rourke for their support and to Sam Spencer for his assistance. Our thanks to Bill Joyner and Ken Campbell for their thoughtful reviews.

REFERENCES

Anderson, J. G., 1986, Implication of attenuation on studies of the earthquake source, in Das, S., Boatwright, J., and Scholz, C., eds., Earthquake Source Mechanics: American Geophysical Union Monograph 37, Washington, D.C., p. 311-318.

Anderson, J. G., Bodin, P., Brune, J., Prince, J., Singh, S., Quaas, R., Onate, M., and Mena, E., 1986, Strong ground motion and source mechanism of the Mexico earthquake of September 19, 1985: Science, v. 233, p. 1043-1049.

Anderson, J. G. and Hough, S. E., 1984, A model for the shape of the Fourier amplitude spectrum of acceleration at high frequencies: Bulletin of the Seismological Society of America, v. 74, p. 1969-1993.

Anderson, J., Quaas, R., Almora, D., Velasco, J. M., Guevara, E., de Pavia, L. E., Gutierrez, A., and Vazquez, R., 1987, Guerrero, Mexico accelerograph array: Summary of data collected in 1985: Institute of Geophysics and Planetary Physics Report GAA-2, University of California at San Diego, La Jolla, CA, 166 p.

Atkinson, G. M., 1984, Attenuation of strong ground motion in Canada: Bulletin of the Seismological Society of America, v. 74, p. 2629-2653.

Baker, G. E. and Langston, C. A., 1987, Source parameters of the 1949 magnitude 7.1 south Puget Sound, Washington, earthquake as determined from long-period body waves and strong ground motions: Bulletin of the Seismological Society of America v. 77, p. 1530-1557.

Bolt, B.A., 1973, Duration of strong ground motion: Proceedings of the Fifth World Conference on Earthquake Engineering, Rome, Italy, v. I, p. 1304-1313.

Boore, D. M., 1983, Stochastic simulation of high-frequency ground motions based on seismological models of the radiated spectra: Bulletin of the Seismological Society of America, v. 73, p. 1865-1884.

Boore, D. M., 1986, Short-period P- and S-wave radiation from large earthquakes: Implications for spectral scaling relations: Bulletin of the Seismological Society of America, v. 76, p. 43-64.

Boore, D. M. and Atkinson, G. M., 1987, Prediction of ground motion and spectral response parameters at hard-rock sites in eastern North America: Bulletin of the Seismological Society of America, v. 77, p. 440-467.

Boore, D. M. and Joyner, W. B., 1984, A note on the use of random vibration theory to predict peak amplitudes of transient signals: Bulletin of the Seismological Society of America, v. 74, p. 2035-2039.

Earthquake Engineering Research Laboratory, 1973, Strong motion earthquake accelerograms: California Institute of Technology, EERL 72-51, v. II, Parts B and U.

Hanks, T. C., 1982, fmax: Bulletin of the Seismological Society of America, v. 72, p. 1867-1879.

Hanks, T. C. and McGuire, R. K., 1981, The character of high-frequency strong ground motion: Bulletin of the Seismological Society of America, v. 71, p. 2071-2095.

Hough, S. E., Anderson, J. G., Brune, J., Vernon III, F., Berger, J., Fletcher, J., Haar, L., Hanks, T. and Baker, L., 1988, Attenuation near Anza, California: Bulletin of the Seismological Society of America, v. 78, p. 672-691.

Ihnen, S. M. and Hadley, D. M., 1986, Prediction of strong ground motion in the Puget Sound region: The 1965 Seattle earthquake: Bulletin of the Seismological Society of America, v. 76, p. 905-922.

Johnson, L. R. and Silva, W., 1981, The effects of unconsolidated sediments upon the ground motion during local earthquakes: Bulletin of the Seismological Society of America, v. 71, p. 127-142.

Joyner, W. and Boore, D.M., 1988, Measurement, characterization, and prediction of strong ground motion, in Von Thun, J.L., ed., Proceedings of Earthquake Engineering and Soil Dynamics II- Recent Advances in Ground Motions Evaluation: American Society of Civil Engineering, Geotechnical Special Publication No. 20, p. 43-103.

Joyner, W., Warrick, R. E. and Fumal, T. E., 1981, The effect of Quaternary alluvium on strong ground motion in the Coyote Lake, California, earthquake of 1979: Bulletin of the Seismological Society of America, v. 71, p. 1333-1349.

Joyner, W., Warrick, R. E. and Oliver, A. A. III, 1976, Analysis of seismograms from a downhole array in sediments near San Francisco Bay: Bulletin of the Seismological Society of America, v. 66, p. 937-958.

Langston, C. A., 1981. A study of Puget Sound strong ground motion: Bulletin of the Seismological Society of America, v. 71, p. 883-903.

Langston, C. A., and Blum, D. E., 1977, The April 29, 1965, Puget Sound earthquake and the crustal and upper mantle structure of western Washington: Bulletin of the Seismological Society of America, v. 67, p. 693-711.

Mohraz, B. J., 1976, A study of earthquake response spectra for different geologic conditions: Bulletin of the Seismological Society of America, v. 66, p. 915-935.

Nuttli, O. W., 1986, Yield estimates of Nevada Test Site explosions obtained from seismic Lg wave: Journal of Geophysical Research, v. 91, p. 2137-2151.

Papageorgiou, A. S. and Aki, K., 1983, A specific barrier model for the quantitative description of inhomogeneous faulting and the prediction of strong ground motion, Part II: Applications of the model: Bulletin of the Seismological Society of America, v. 73, p. 953-978.

Seed, H. B. and Idriss, I. M., 1970, Soil moduli and damping factors for dynamic response analysis, Earthquake Engineering Center, University of California, Berkeley, Report No. EERC 70-10.

Seed, H. B., Ugas, C. and Lysmer, J., 1976, Site-dependent spectra for earthquake-resistant design: Bulletin of the Seismological Society of America, v. 66, p. 221-243.

Shakal, A. F. and Toksoz, M. N., 1980, Amplification and attenuation of site structure: Puget Sound strong motion [abs.], Earthquake Notes, v. 50, p. 20.

Shannon and Wilson, Inc., and Agbabian Associates, 1978, Geotechnical and strong motion earthquake data from U.S. accelerograph stations: NUREG/CR-0985, v. 4.

Silva, W. J., 1976, Body waves in a layered anelastic solid: Bulletin of the Seismological Society of America, v. 66, p. 1539-1554.

Silva, W. J. and Darragh, R. B., 1990, Engineering characterization of strong ground motion recorded at rock sites: Prepared by Woodward-Clyde Consultants, Electric Power Research Institute Final Report (in press).

Silva, W. J., Darragh, R. B., Green, R., and Turcotte, F. T., 1989, Spectral characteristics of small magnitude earthquakes with applications to western and eastern North American environments: Surface motions and depth effects: U.S. Army Engineers Waterways Experiment Station Miscellaneous Paper GL-89-16, 84 p.

Silva, W. J. and Green, R. K., 1988, Magnitude and distance scaling of response spectral shapes for rock sites with applications to North American tectonic environment: Earthquake Spectra, v. 5, p. 591-624.

Silva, W. J. and Lee, K. 1987, WES RASCAL Code for synthesizing earthquake ground motions: State-of-the-Art for Assessing Earthquake Hazards in the United States, Report 24: U.S. Army Corps of Engineers Waterways Experiment Station, Miscellaneous Paper S-73-1, 120 p.

Silva, W. J., Turcotte, F. T. and Moriwaki, Y., 1988, Soil response to earthquake ground motions: Prepared by Woodward-Clyde Consultants, Electric Power Research Institute Final Report NP-5747.

Toro, G. R. and McGuire, R. K., 1987, An investigation into earthquake ground motion characteristics in eastern North America: Bulletin of the Seismological Society of America, v. 77, p. 468-489.

Toro, G. R., McGuire, R. K., and Silva, W. J., 1988, Engineering model of earthquake ground motion for eastern North America: Prepared by Risk Engineering, Inc., Electric Power Research Institute Final Report NP-6074.

Washington Public Power Supply System, 1974, Preliminary Safety Analysis Report: Supply System Projects Nos. 3 and 5.

Washington Public Power Supply System, 1986, Final Safety Analysis Report: Supply System Nuclear Project No. 3, Volume 7, Appendix 2.5.k.

Table 1

EARTHQUAKE SOURCE AND WAVE PROPAGATION PARAMETERS

Parameters	Pacific Northwest
ρ_o	2.7 g/cm^3
β_o	3.2 km/sec (2.0 mi/sec)
κ	0.02 sec
Q(f)	$150(f)^{0.60}$ (Nuttli, 1986)
$\Delta\sigma$	100 bars
M_o	log M_o (dyne-cm) = 1.5 M + 16.1
Amplification Factors	See Boore (1986)
Geometrical Attenuation	R^{-1}
Source Duration	f_c^{-1}
$(f_c)^3$	$\beta^3\Delta\sigma/8.44\ M_o$

TABLE 2

OBSERVED AND PREDICTED MEDIAN PEAK HORIZONTAL ACCELERATIONS

Station	Event	Depth in km (mi)	Epicentral Distance in km (mi)	Magnitude	Stress Parameter (bars)	PGA (g)
OHT	13 April 1949	49 (30.6)	5 (3.1)	M 7.1	100	0.16, 0.28 (obs) 0.18 (model)
OHT	29 April 1965	60 (37.5)	69 (43.1)	M 6.5	100	0.20, 0.14 (obs) 0.07 (model)
FED	29 April 1965	60 (37.5)	21 (13.1)	M 6.5	100	0.07, 0.07 (obs) 0.07 (model)
FED	CASCADIA	40 (25.0)	57 (35.6)	M 8.0	100	0.11 (rock, model) 0.17 (soil, model)

FIGURE CAPTIONS

Figure 1. Band-Limited-White-Noise ground motion model.

Figure 2. The average 5% spectral shape of the M 7.9 1985 Michoacan, Mexico earthquake as computed from four rock sites in the Guerrero strong motion network (dashed line). The dotted lines represent the maximum and minimum of the eight horizontal components. The solid line is the BLWN-RVT model shape for a M 7.9 event at a distance of 16 km using a κ of 0.05 sec.

Figure 3. Soil profile used in comparison of site response analysis between time domain estimates of peak shear-strain (SHAKE) (thin solid line) and RVT estimates of peak shear-strain (heavy solid line).

Figure 4. Plot of shear-strain dependency of shear-wave damping and shear modulus used in analyses (modified after Seed and Idriss, 1970).

Figure 5. Plot of synthetic outcrop motion for a M 6.5 earthquake at a hypocentral distance of 8.5 km (top trace), output time history resulting from SHAKE analysis (middle trace), and time history resulting from frequency domain RVT analysis (bottom trace).

Figure 6. Plot of (5%) absolute acceleration response spectra resulting from the SHAKE site-response analysis (dotted line) and RVT estimates (solid line). Also shown is the RVT estimate of oscillator response for the rock outcrop (control) motion (dashed line).

Figure 7. Geologic profiles for OHT and FED.

Figure 8. The observed and predicted acceleration response spectral shape of the 13 April 1949 earthquake for the Highway Test Laboratory (OHT) site.

Figure 9. The observed and predicted acceleration response spectral shape of the 29 April 1965 earthquake for the Highway Test Laboratory (OHT) site.

Figure 10. The observed and predicted acceleration response spectral shape of the 29 April 1949 earthquake for the Federal Building (FED) site.

Figure 11. Predicted acceleration response spectra of a hypothetical M 8 Cascadia earthquake for a hypothetical hard rock site and for the Federal Building (FED) site.

Figure 12. Predicted accelerograms for a hypothetical M 8 Cascadia earthquake at a hard rock site (top) and at the Federal Building (FED) site (bottom) at a rupture distance of 70 km.

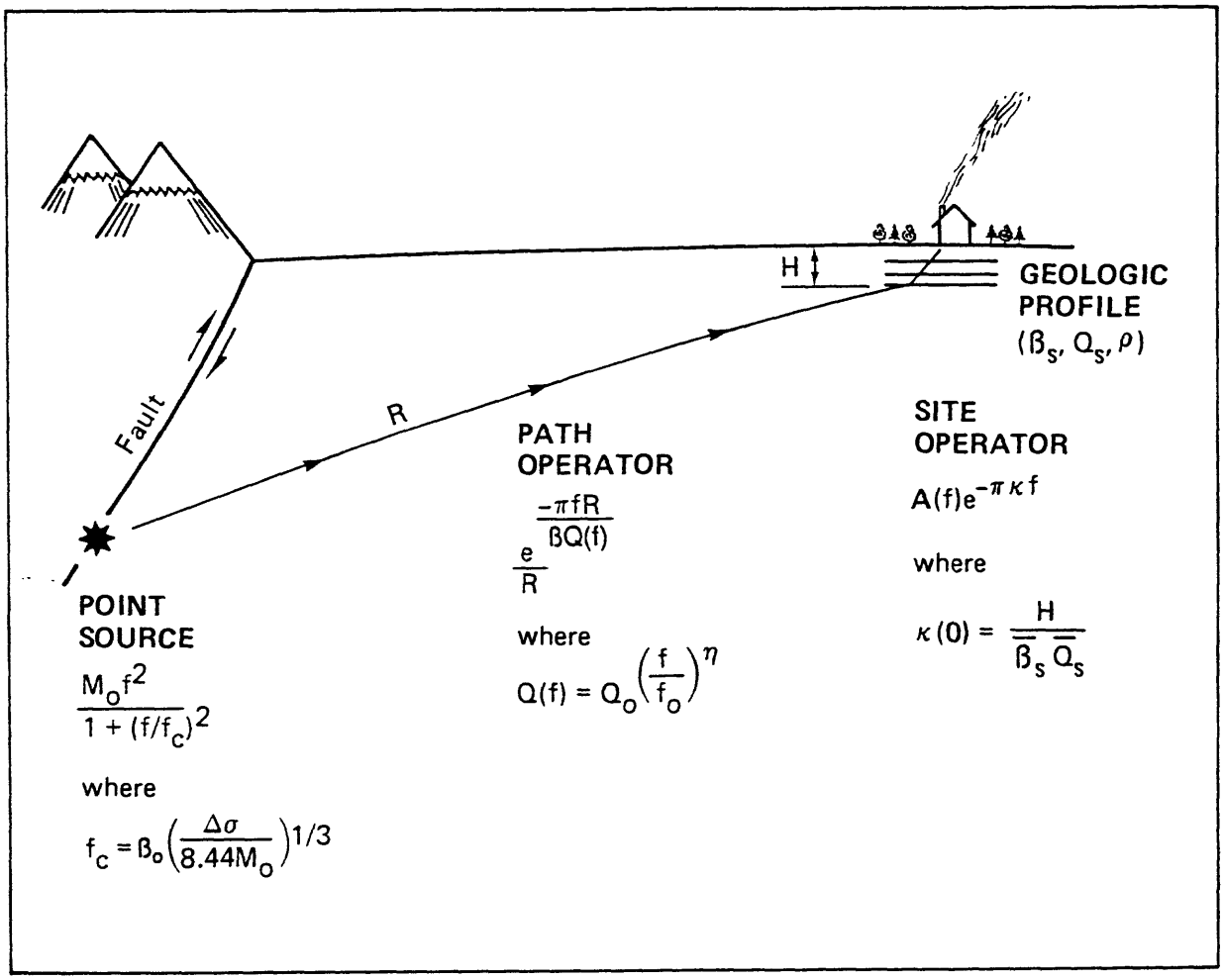
H
GEOLOGIC PROFILE
(β_s, Q_s, ρ)
Fault
R
PATH OPERATOR
$\frac{e^{\frac{-\pi f R}{\beta Q(f)}}}{R}$
where
$Q(f) = Q_o\left(\frac{f}{f_o}\right)^{\eta}$
SITE OPERATOR
$A(f)e^{-\pi \kappa f}$
where
$\kappa(0) = \frac{H}{\overline{\beta}_s \overline{Q}_s}$
POINT SOURCE
$\frac{M_o f^2}{1 + (f/f_c)^2}$
where
$f_c = \beta_o\left(\frac{\Delta\sigma}{8.44 M_o}\right)^{1/3}$

Figure 1

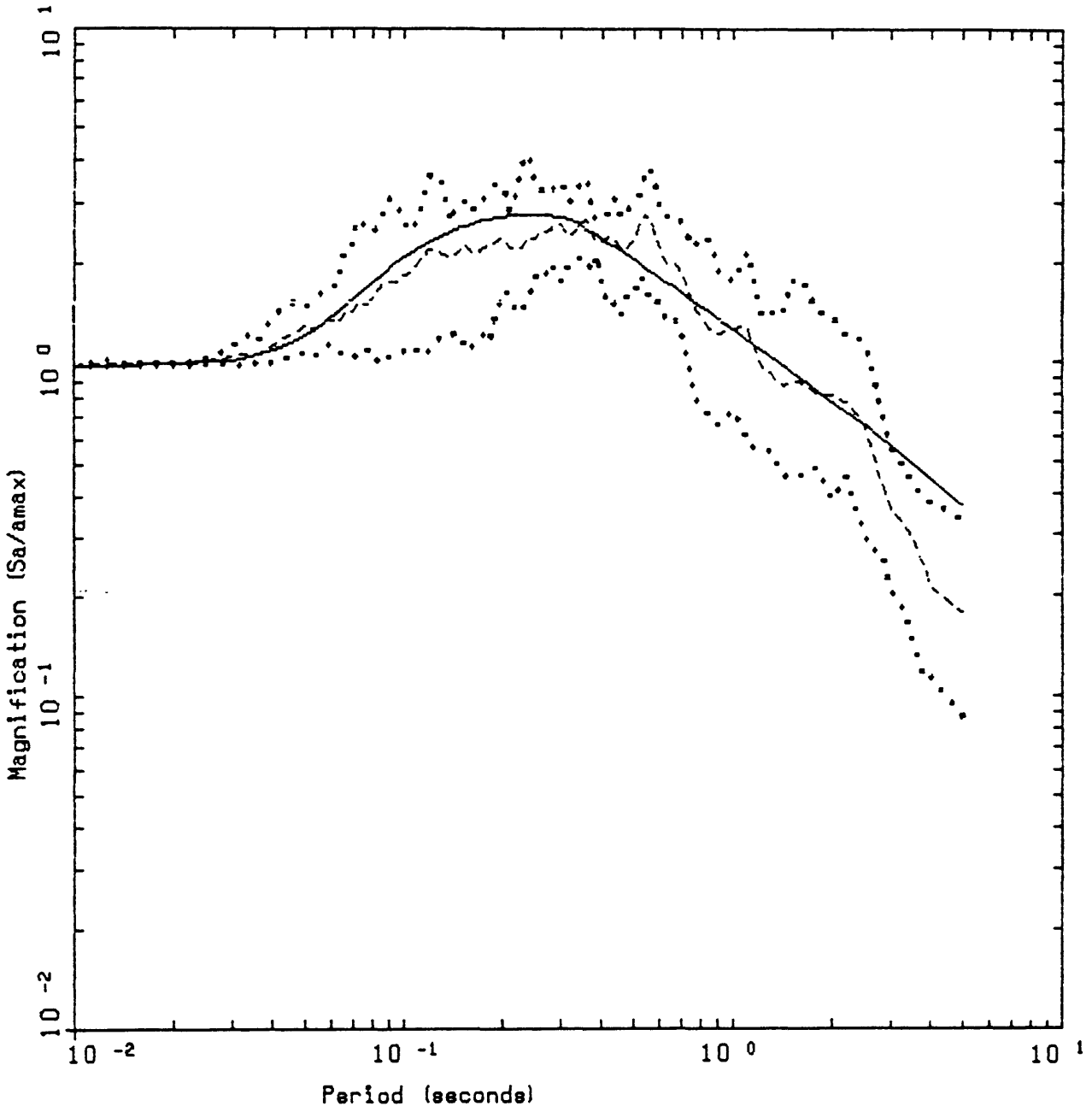
Magnification (Sa/amax)
10 1
10 0
10 -1
10 -2
10 -2
10 -1
10 0
10 1
Period (seconds)

Figure 2

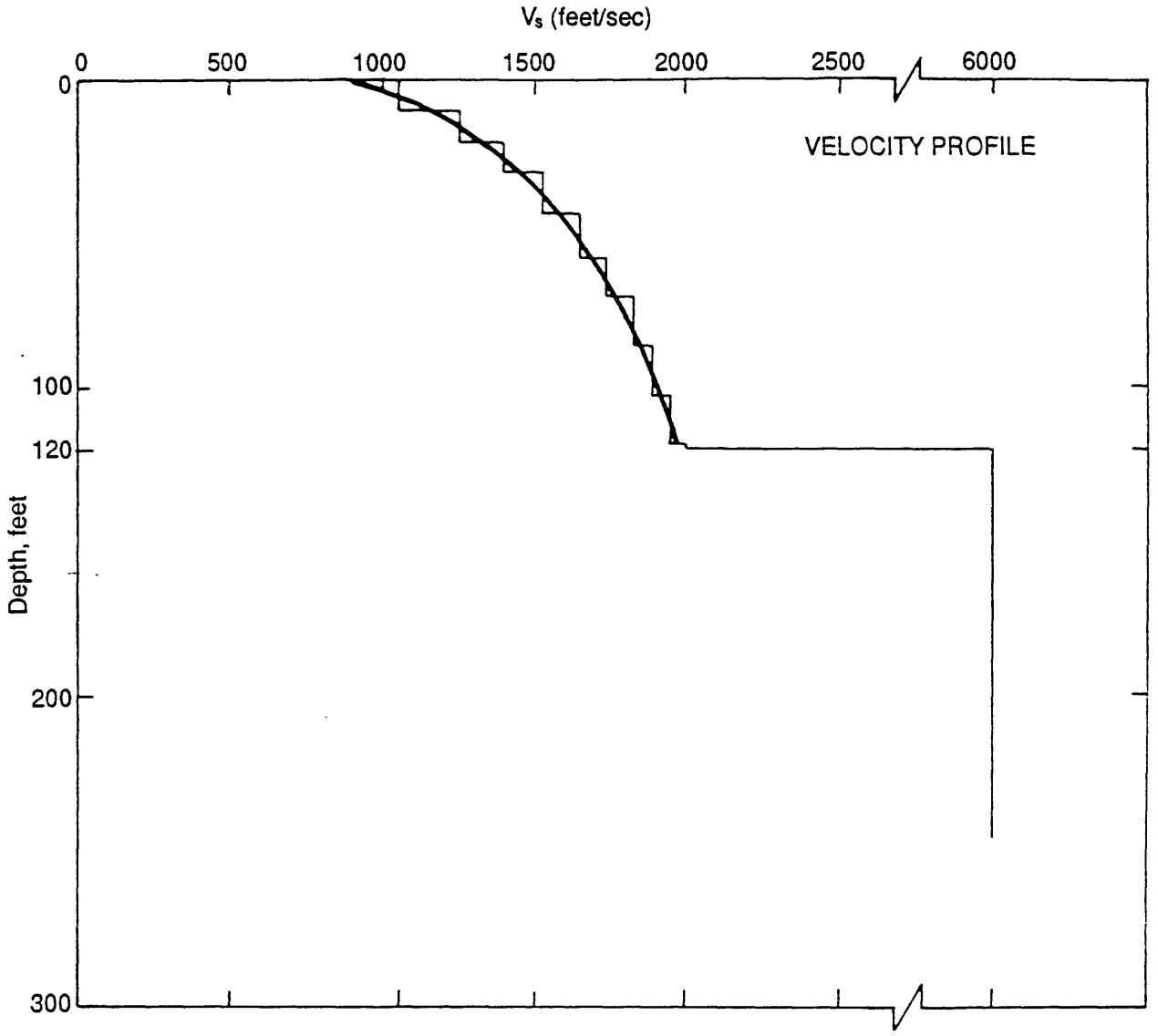
Vs (feet/sec)
0
500
1000
1500
2000
2500
6000
VELOCITY PROFILE
Depth, feet
0
100
120
200
300

Figure 3

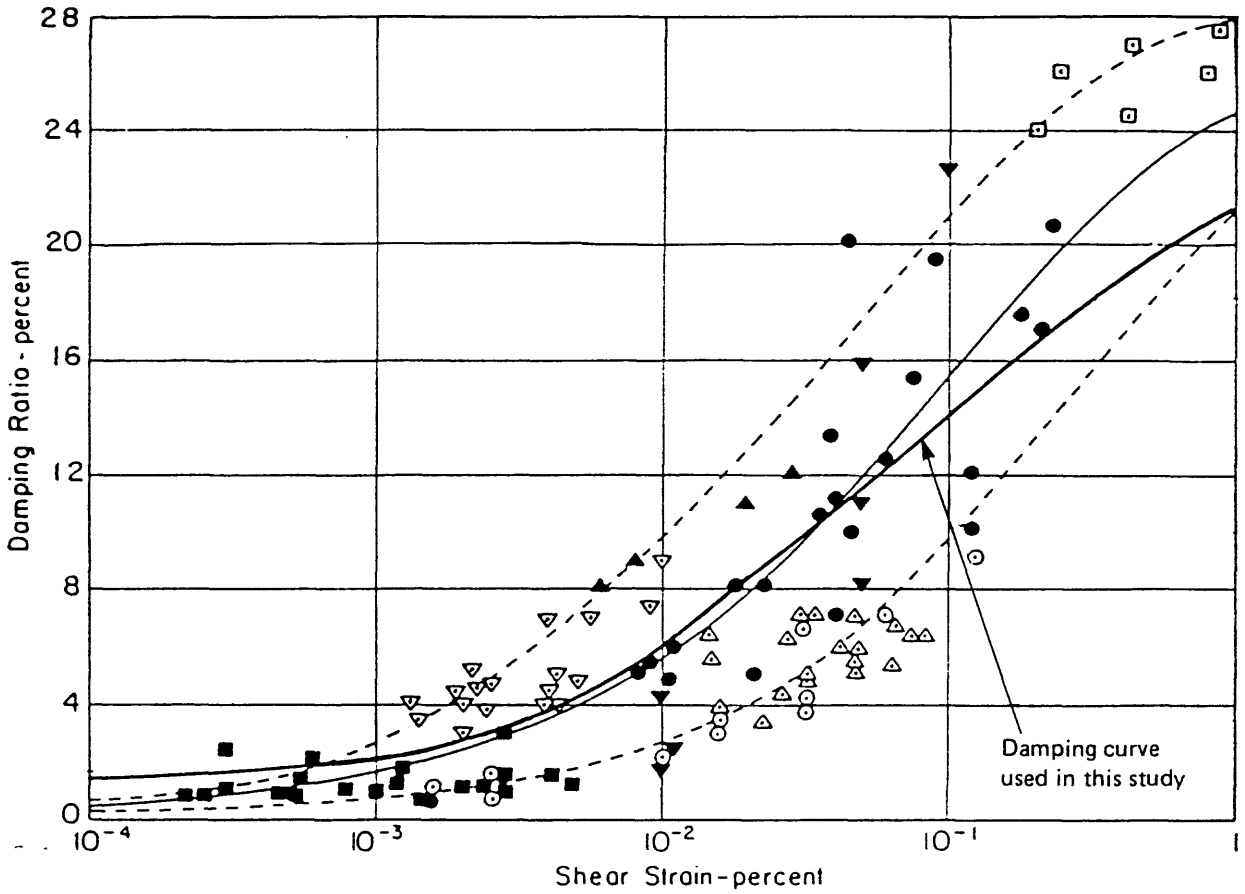
28
24
20
16
12
8
4
0
Damping Ratio - percent
10^{-4}
10^{-3}
10^{-2}
10^{-1}
1
Shear Strain - percent
Damping curve
used in this study

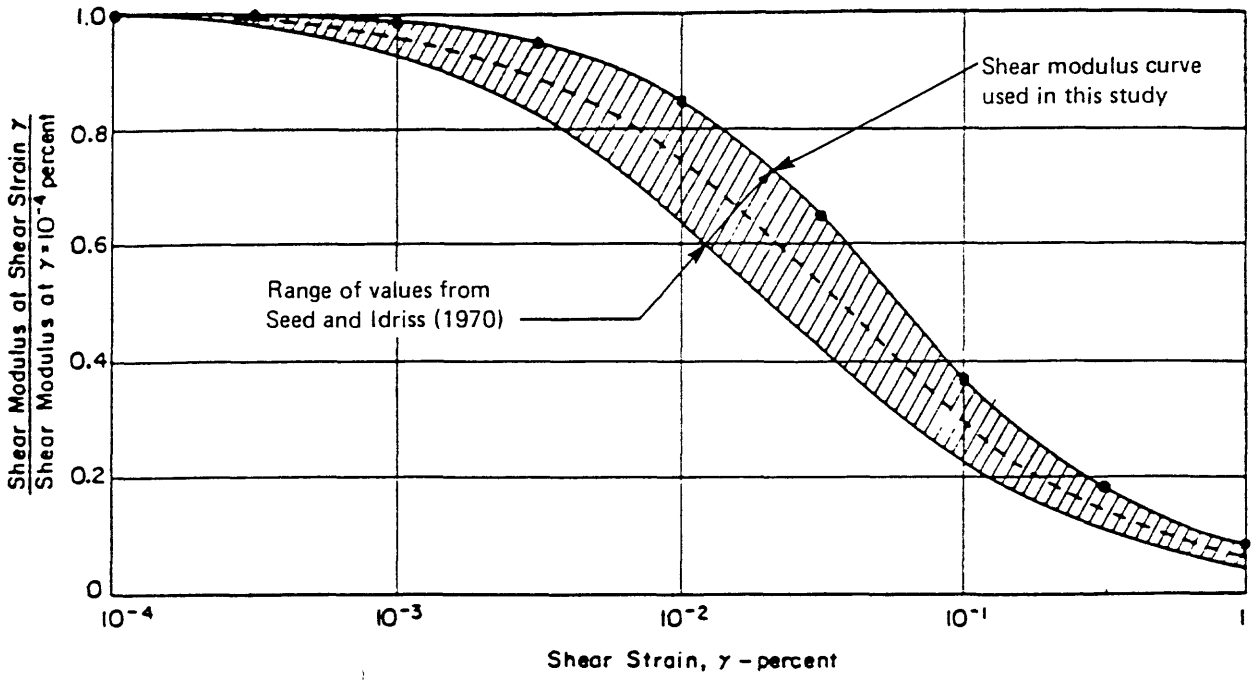
1.0
0.8
0.6
0.4
0.2
0
Shear Modulus at Shear Strain γ / Shear Modulus at γ = 10⁻⁴ percent
Shear modulus curve
used in this study
Range of values from
Seed and Idriss (1970)
10^{-4}
10^{-3}
10^{-2}
10^{-1}
1
Shear Strain, γ - percent

Figure 4

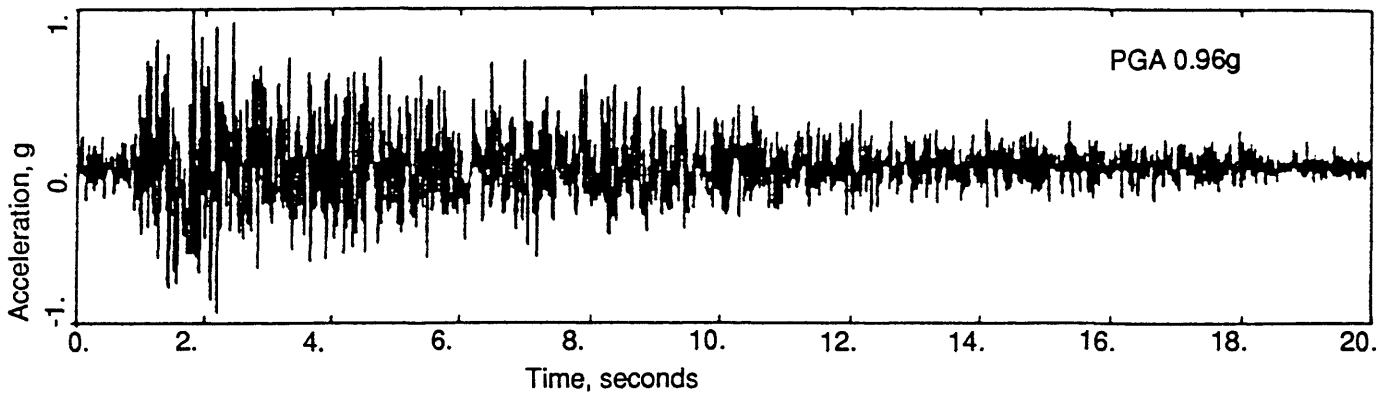
PGA 0.96g
Acceleration, g
1.
0.
-1.
0.
2.
4.
6.
8.
10.
12.
14.
16.
18.
20.
Time, seconds

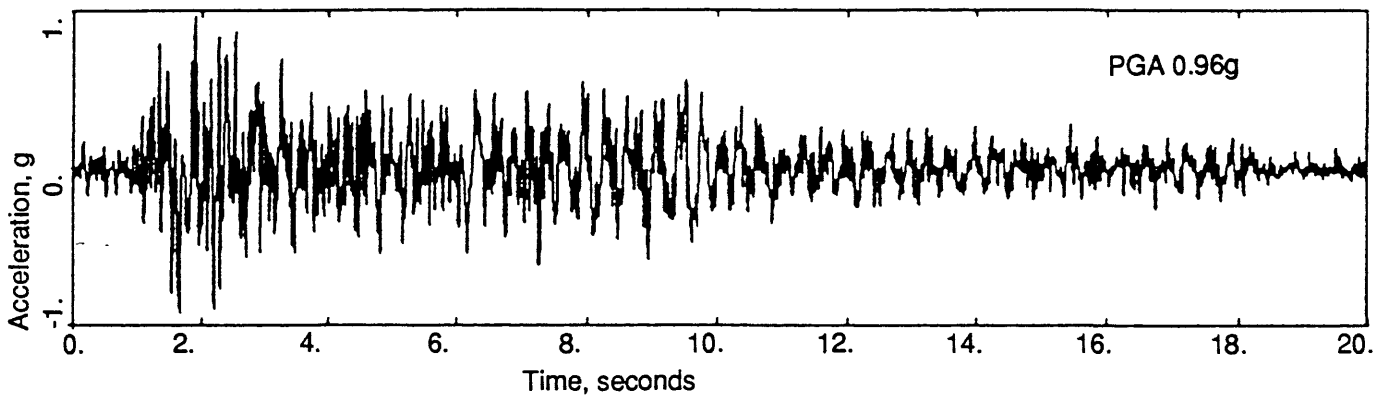
PGA 0.96g
Acceleration, g
1.
0.
-1.
0.
2.
4.
6.
8.
10.
12.
14.
16.
18.
20.
Time, seconds

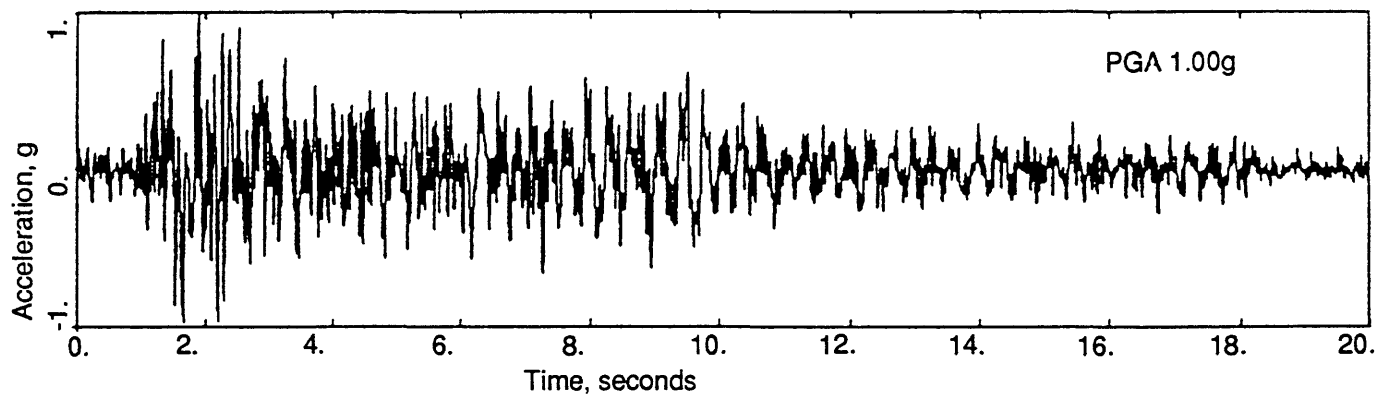
PGA 1.00g
Acceleration, g
1.
0.
-1.
0.
2.
4.
6.
8.
10.
12.
14.
16.
18.
20.
Time, seconds

Figure 5

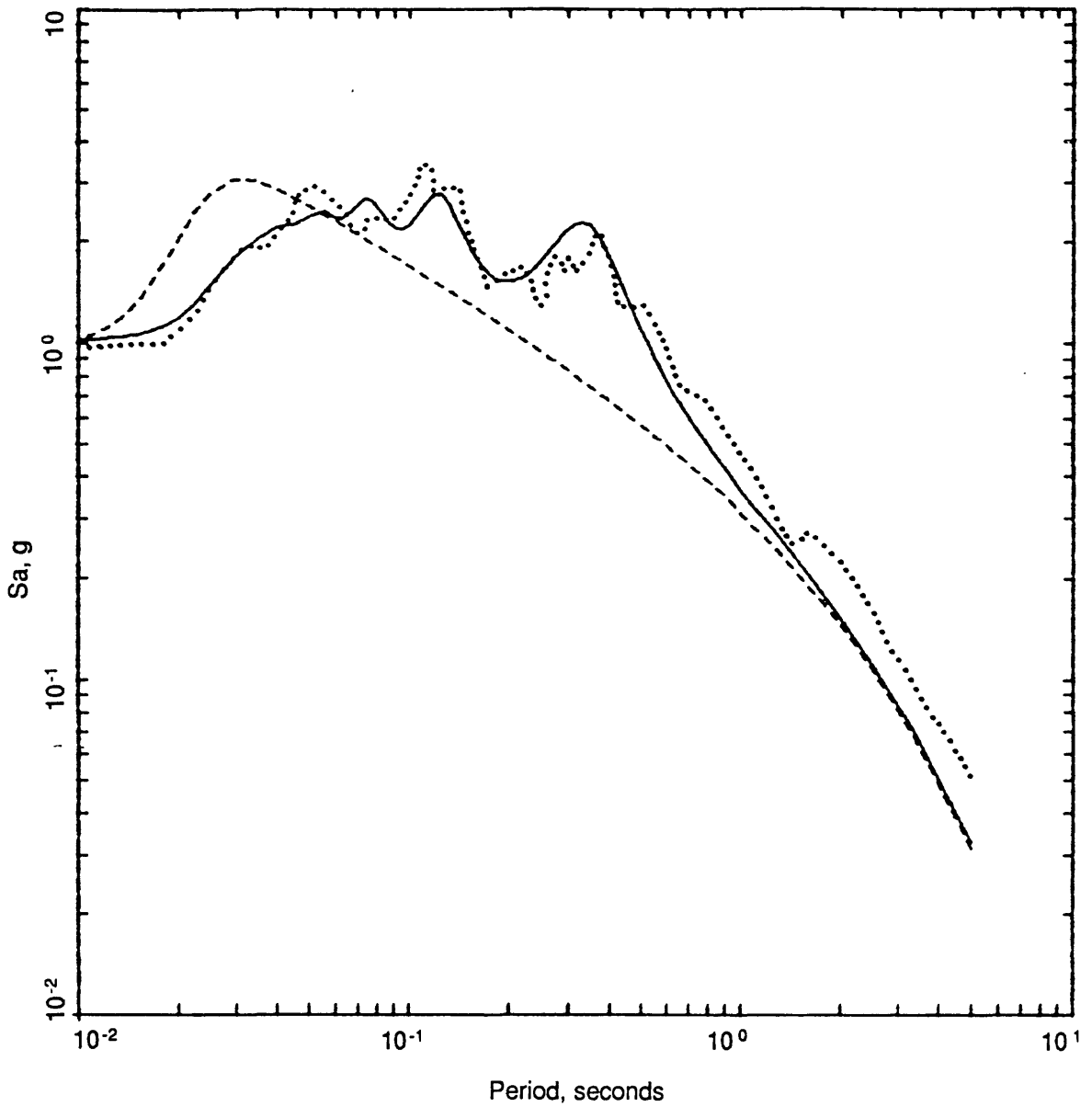

Figure 6

HIGHWAY TEST LAB, OLYMPIA (OHT)

DEPTH (m)	GEOLOGY	DESCRIPTION	β_s (m/sec)	ρ (g/cm^3)	Q_s
3	Fill	Loose sand	142	2.1	10.0
12	Glacial Fluvial Deposits	Medium dense fine to medium sand	142–230	2.0–2.1	10.0
41	Glacio-lacustrine Deposits	Interbedded very stiff to hard fine sandy silt and very dense silty fine to medium sand	230–330	1.9–2.0	10.0
		Very dense fine to medium sand	363–685	1.9–2.1	10.0–20.0
131*	— — — Bottom of profile used in modeling — — —				
144	Glacio-lacustrine Desposits(?)	Interbedded hard silty clay and very dense silty fine sand	No measure-ments	—	—
156					

FEDERAL OFFICE BUILDING SEATTLE (FED)

DEPTH (m)	GEOLOGY	DESCRIPTION	β_s (m/sec)	ρ (g/cm^3)	Q_s
0	Fill	Loose to medium clayey, silty fine sand	150–200	1.5	10.0
7	Quaternary Glacial Drift	Very dense, silty gravelly fine sand	420	1.5	10.0
16		Very dense, silty, clay with gravel	430	1.5	10.0
23		Hard silty clay with some gravel	430–500	1.5–1.7	10.0
47		Very dense silty, sandy fine gravel and silty gravelly fine to coarse sand with some cobbles	610–1006	1.8–2.0	10.0–31.3
122					

Figure 7

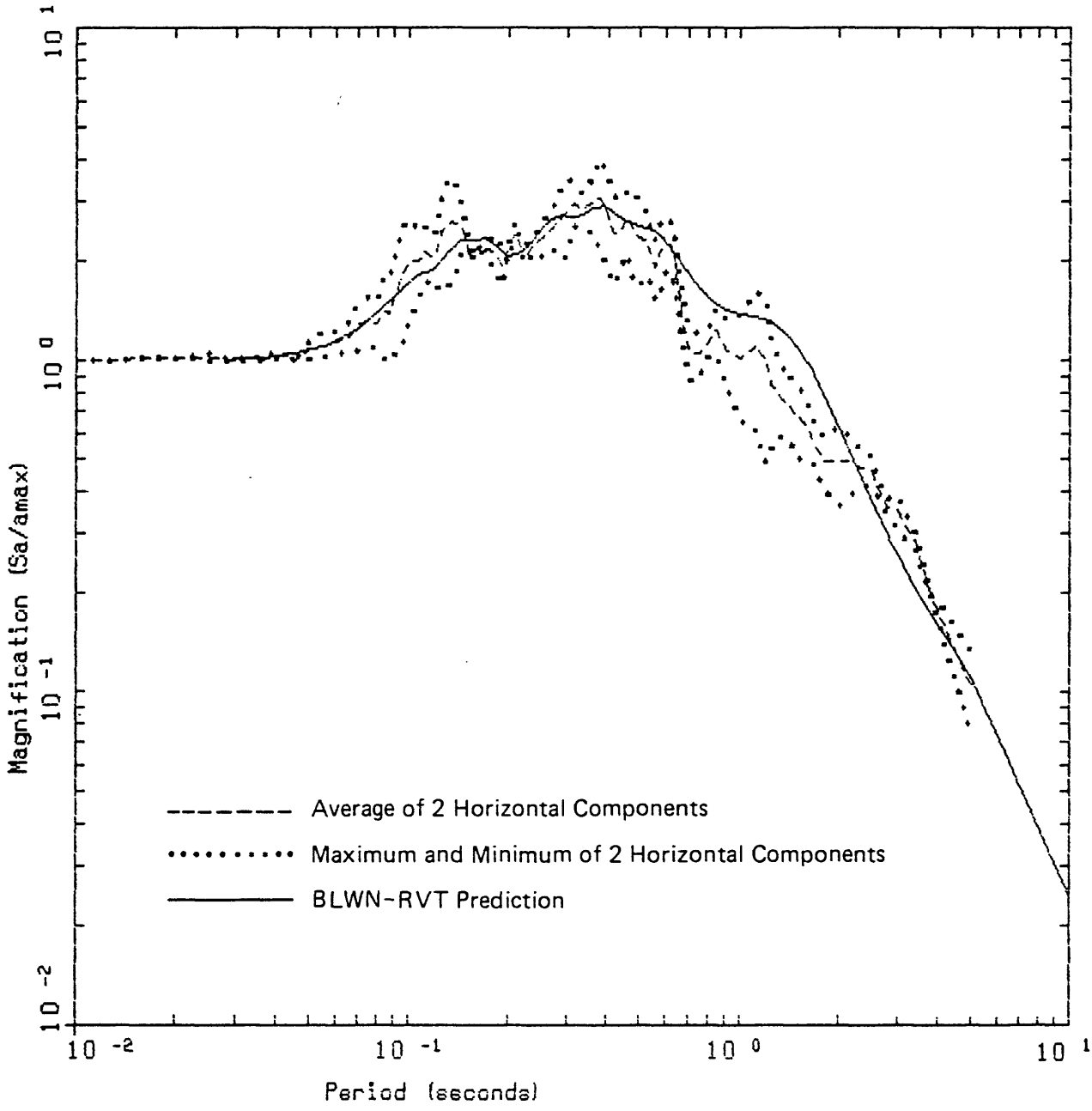
Magnification (Sa/amax)
10 1
10 0
10 -1
10 -2
10 -2
10 -1
10 0
10 1
Period (seconds)
Average of 2 Horizontal Components
Maximum and Minimum of 2 Horizontal Components
BLWN-RVT Prediction

Figure 8

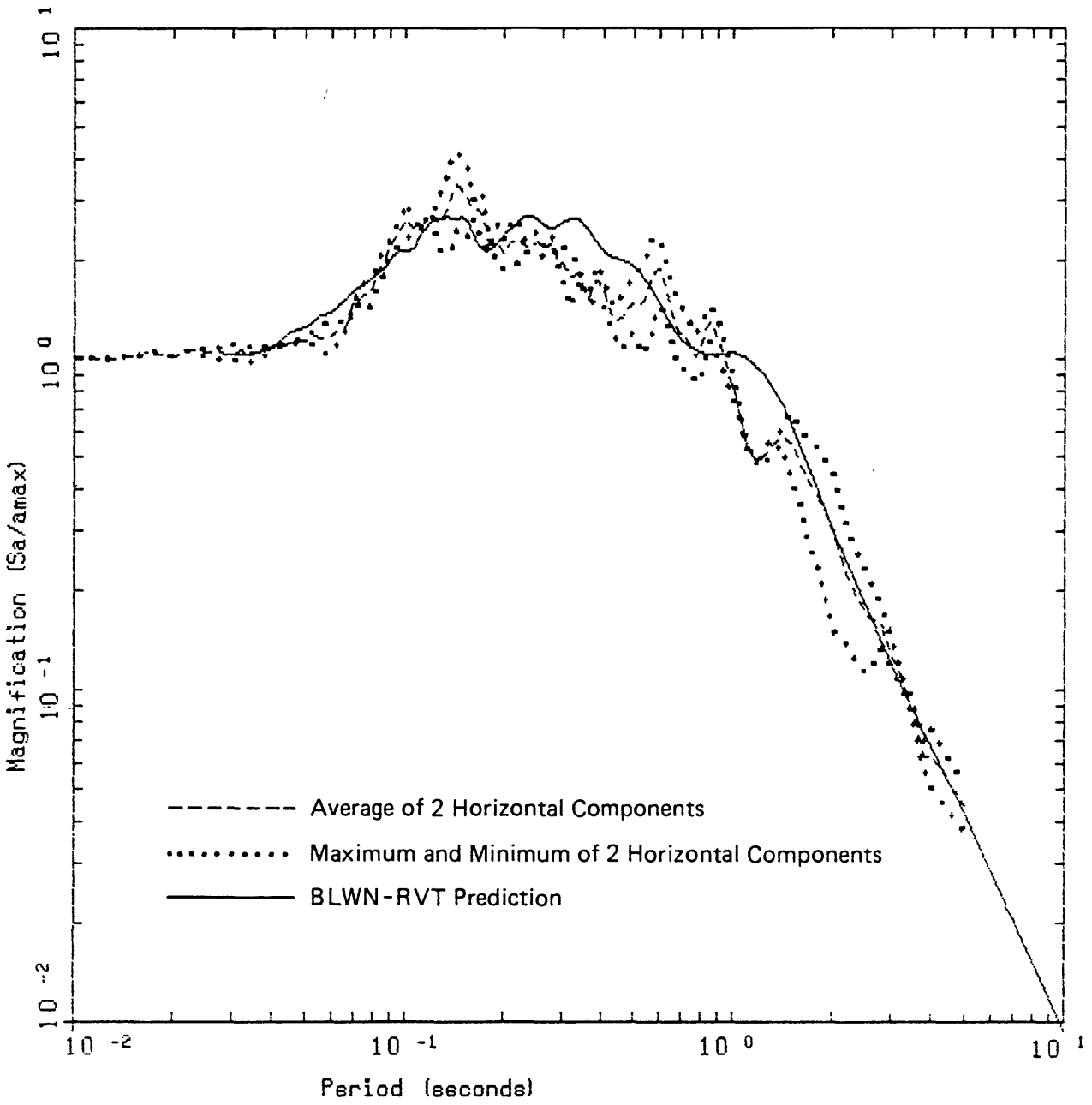
Magnification (Sa/amax)
10 1
10 0
10 -1
10 -2
10 -2
10 -1
10 0
10 1
Period (seconds)
Average of 2 Horizontal Components
Maximum and Minimum of 2 Horizontal Components
BLWN-RVT Prediction

Figure 9

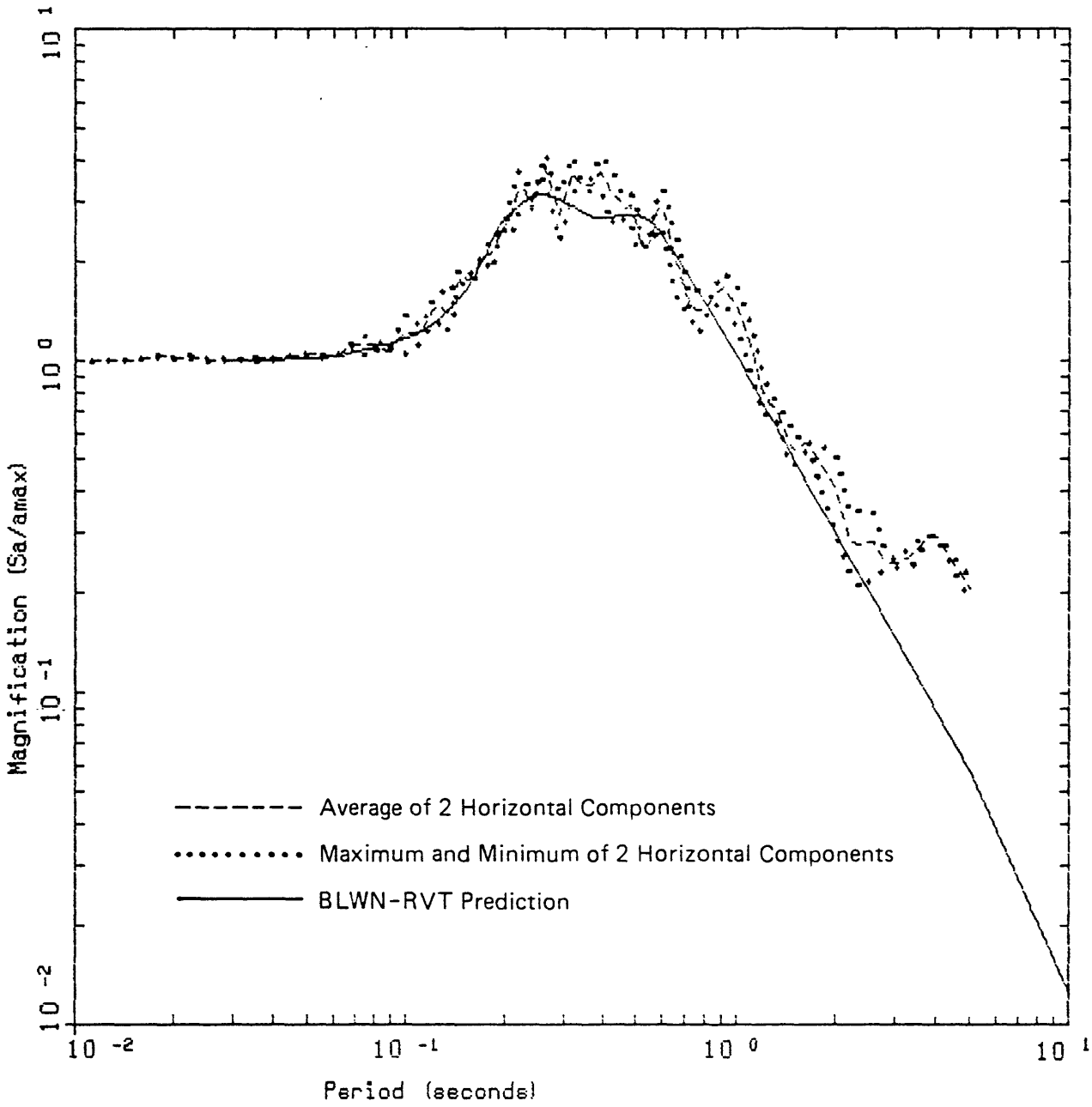
Magnification (Sa/amax)
10 1
10 0
10 -1
10 -2
10 -2
10 -1
10 0
10 1
Period (seconds)
Average of 2 Horizontal Components
Maximum and Minimum of 2 Horizontal Components
BLWN-RVT Prediction

Figure 10

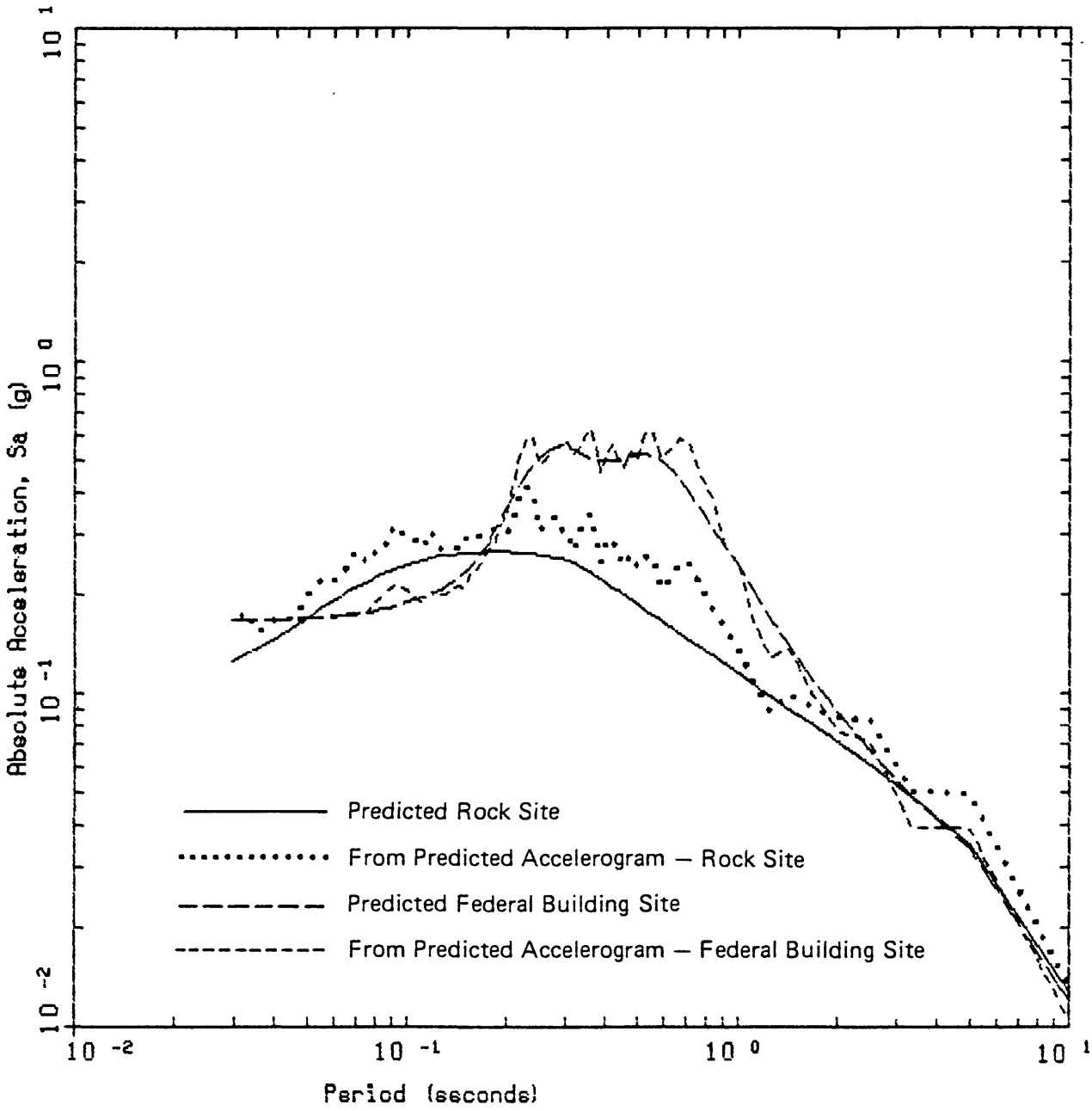
Absolute Acceleration, Sa (g)
10 1
10 0
10 -1
10 -2
10 -2
10 -1
10 0
10 1
Period (seconds)
Predicted Rock Site
From Predicted Accelerogram — Rock Site
Predicted Federal Building Site
From Predicted Accelerogram — Federal Building Site

Figure 11

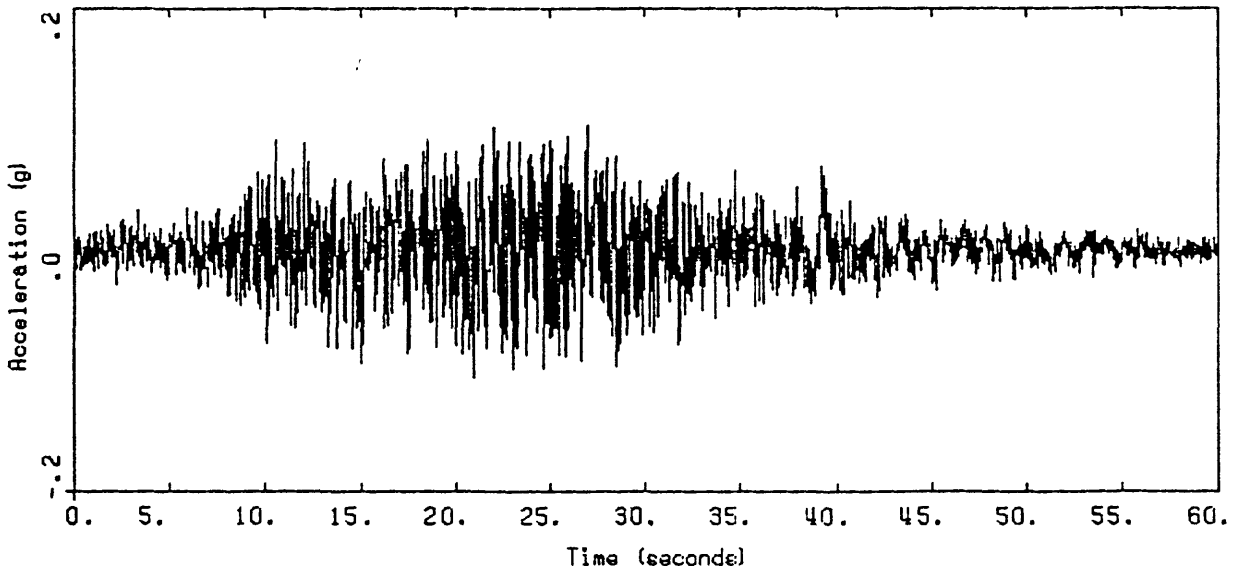
.2
.0
-.2
Acceleration (g)
0.
5.
10.
15.
20.
25.
30.
35.
40.
45.
50.
55.
60.
Time (seconds)

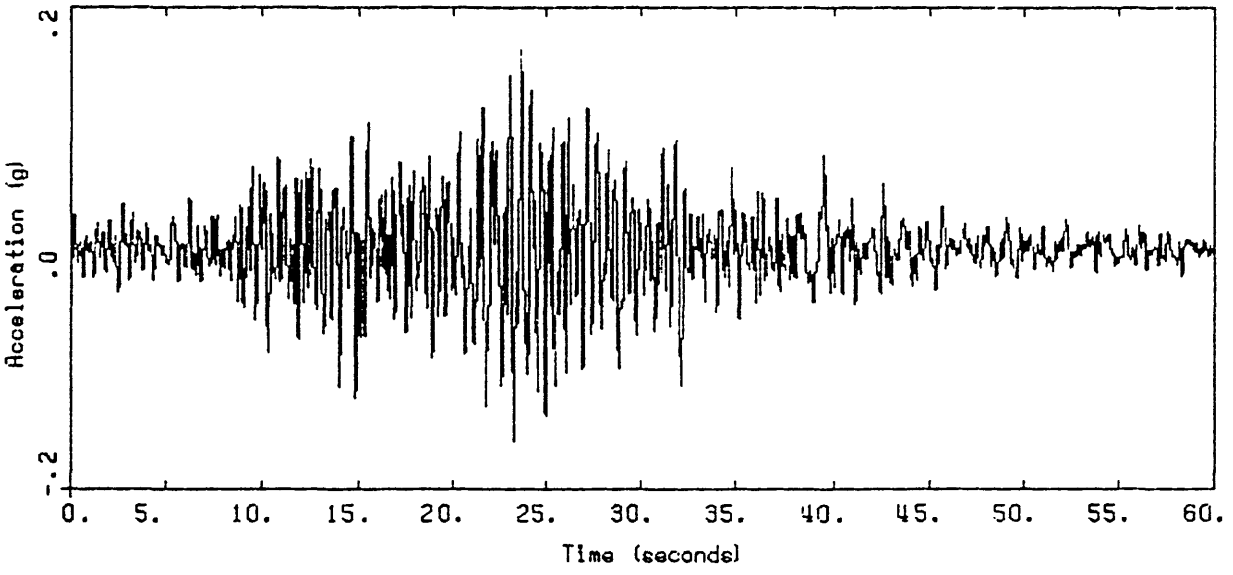
.2
.0
-.2
Acceleration (g)
0.
5.
10.
15.
20.
25.
30.
35.
40.
45.
50.
55.
60.
Time (seconds)

Figure 12